Aerodynamic Performance Optimization of Smart Wing Using SMA Actuator

Dileep E.[1], Nebish M.[2] and Loganathan V.[3]
[1]Nehru Institute of Engineering and Technology, Coimbatore, INDIA
[2]RVS College of Engineering and Technology, Coimbatore, INDIA
[3]Government College of Engineering, Salem, INDIA

Abstract

Airplanes found today in commercial, private or military use possess fix wings that allow them to fly. The different shapes of wings, camber angles, textures among other characteristics gives the aircraft its own aerodynamic properties. These properties allow the aircraft to fulfill the specific task for which it was intended. However, new technology and development has pushed forward the idea of a wing that could have different aerodynamics properties by changing its form and shape. This would make it able to adapt itself to different flight conditions. The main objective of the current research work is to improve the aerodynamic performance of an experimental aircraft wing that operates at various cruise conditions. The improvement is realized through viscous drag reduction by promoting a large laminar flow run on the upper surface of the wing. To achieve this aerodynamic ability, regardless of the flow conditions, the wing upper surface is subject to controlled and well-studied deformation (in-flight morphing) to keep the drag at its lowest possible value. In the current research work, the wing is equipped with new morphing actuation mechanism hardware with suitably designed controllers. The purpose of this experiment was to develop a mechanism using Shape Memory Allows (SMA) to vary the camber thickness of the wing. The airfoil used in this experiment was a NACA0021. The fabrication of morphing wing has been done and the two-dimensional analysis, using computational fluid dynamics (CFD) and aerodynamic tests were conducted in an open-circuit wind tunnel for this morphing wing. The tests were carried out for this morphing wing to determine the lift to drag ratio at various angles of attack. Then the results obtained by CFD and experimental have been discussed.

Keywords: Airfoil, morphing wing, CFD, SMA, gambit, fluent, wind tunnel, composite, actuator, thin airfoil theory, lift, drag, lift to drag ratio, pressure distribution, velocity distribution, contours.

Introduction

Recent advances in adaptive structures and smart materials have created a great deal of interest in aircraft applications. One of the more intriguing applications is a "morphing aircraft" that could change its shape during flight to efficiently Perform multiple, dissimilar tasks. Several researches Programs are underway to help mature morphing technologies such as hinge-less control surfaces, variable wing twist, and seamless variable camber[1]. Morph can be defined as "to cause something to change its outward appearance". When we talk about a morphing wing we refer to a wing that is able to transform its shape or any other characteristic that can affect its aerodynamic properties. Experts refer to it as a wing that can sense its environment and adapt its shape to perform optimally in a wide range of flight conditions. Each aircraft today has a wing that matches the purpose for its use. By changing the area of the wing, they are able to modify the amount of lift that is needed to either go on a fast attack or simply glide for energy saving.

An airplane with this kind of technology would be able to perform different roles that may seem paradoxical at first. A commercial plane with this morphing technology could be able to adapt its wings for high lift during takeoff, extend them fully for optimum cruising, and fold them lightly for efficient descent and change them back to high lift for landing. With the present technology, the mechanisms that would allow this kind of capability are impractical in the sense that the weight of the wing would increase considerably as well as the cost effectiveness[2]. The optimized airfoil is shown in figure 1. Smart materials instead, could prove useful in the design of these new flight control mechanisms. Shape Memory Alloys such as Nitinol are able to expand and contract with changes in temperature. These smart materials would eliminate the weight problem and could make the morphing mechanisms more practical. The objective of this research is to develop a concept for a working mechanism using the smart material Nitinol that helps to increase the camber thickness of the airfoil. This increase in camber would allow gaining higher lift to drag ratio and more efficient aerodynamics[3].

Shape Memory Alloys: Shape memory alloys (SMA) having the composition in the range of 53-55% of nickel. SMA's have been widely employed as actuators and sensors in applications including smart structures, biomedical devices, and robotics. SMA's have the ability to return to a predetermined shape when

cooled. When an SMA is hot, or above its transformation temperature, it has very low yield strength and can be deformed quite easily into any new shape which it will retain[4].

However, when the material is heated above its transformation temperature it undergoes a change in crystal structure which causes it to return to its original shape. If the SMA encounters any resistance during this transformation, it can generate extremely large forces[5]. This phenomenon provides a unique mechanism for remote actuation.

Nitinol has the resistance properties which enable it to be actuated electrically by joule heating. When an electric current is passed directly through the wire, it can generate enough heat to cause the phase transformation. In most cases, the transition temperature of the SMA is chosen such that room temperature is well below the transformation point of the material[6]. Only with the intentional addition of heat can the SMA exhibit actuation. In essence, Nitinol is an actuator, sensor, and heater all in one material.

Nitinol is available in the form of wire, rod and bar stock, and thin film. SMA has a low temperature and a high temperature phase and its unique characteristics arise from change its phase[7]. The phase change is between two solid phases and involves arrangement of atoms with crystal lattice.

The internal structure is different at different temperatures. The low temperature phase is called martensite, with a highly twinned martensite and high temperature phase is called austenite phase with a body centered cubic structure.

The martensite transformation phase starts at Martensite start temperature which is denoted by M_s and ends at martensite finish temperature which is denoted by M_f. The austenite transformation phase is starts with austenite start temperature which is denoted by A_s and ends with austenite finish temperature A_f. The recovery of the SMAs begins at A_s and ends at A_f[8].

Morphing Wing Model: The main concept proposed here was to increase the camber thickness. To increase thickness we are using a flexible skin at the upper surface and a rigid skin in the lower surface of the airfoil. Here the rigid skin is made up of aluminum and the flexible skin is of twill woven hybrid carbon Kevlar composite[9]. This material is chosen because it has a high stiffness and makes a uniform span wise deformation. Mounted on the rigid part, the flexible skin was attached rigidly at 1% chord below the airfoil leading, covering the upper surface of the airfoil.

As depicted in figure 1 the actuators are placed at the 25% c and 47.6% c of the airfoil. The dimensions of the airfoil that we have chosen were chord length of 16 cm and the span of 25 cm. The SMA wire contraction and expansion, depending on temperature change were transformed to vertical displacements

up to 8 mm at actuating points. These displacements will result in the increase in camber thickness and leads high L/D ratio. The figure 2 is the airfoil that is fabricated using the teak wood and the space between them is for fixing the mechanism for actuating. The figure 3 shown below is a designed model of airfoil. The figure 4 shows clearly the mechanism that was used to morph the airfoil upper surface.
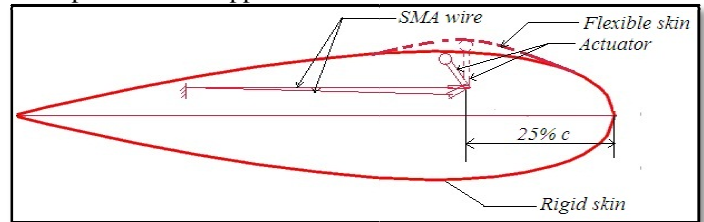

Figure-1
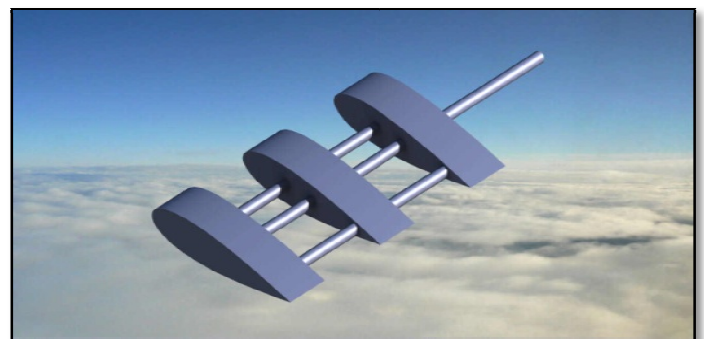**Airfoil Optimized**

Figure-2
Fabricated Airfoil

Figure-3
Designed Airfoil

Figure-4
Fabricated Mechanism

Methodology

Experimental Analysis: The aerodynamic tests were carried out in an open-circuit subsonic wind tunnel at a speed of 0.6 mach (225 m/s). The test section of the wind tunnel is of 300 mm × 300 mm and 600 mm long. The figure 5 illustrates the subsonic wind tunnel which is used to analyze the morphed and un-morphed airfoils. The figure 6 illustrates the un-morphed and morphed airfoils. The airfoils are kept inside the wind tunnel test section to calculate the lift and drag by using a sensor which is attached to the test section of the wind tunnel.

Figure-5
Wind tunnel

Figure-6
Un-Morphed and Morphed Airfoils

The airfoil is kept inside the wind tunnel test section and the lift and drag values of the airfoil are noted by using the sensors by varying the angle of attack up to 25˚ in the increments of +5˚. From the lift and drag values the coefficient of lift and coefficient of drags are calculated by using the formulas

$$C_L = \frac{L}{\frac{1}{2}\rho V^2} \qquad C_D = \frac{D}{\frac{1}{2}\rho V^2}$$

CFD Analysis: The airfoil is analyzed by using the Gambit Fluent platform and the required values are noted down. The profile of the airfoil is drawn by using the coordinates in the Gambit. The coordinates was calculated using the following formula:

$$y_t = \pm 5ct \left[\begin{array}{l} 0.2969 \ \sqrt{\xi} - 0.12605 \ \xi - \\ 0.3516 \ \xi^2 + 0.2843 \ \xi^3 - 0.1015 \ \xi^4 \end{array} \right]$$

Here t represents the maximum thickness expressed as a fraction of the chord and ξ is calculated by using the following formula:

$$\xi \quad = \quad \frac{X}{c}$$

The leading-edge radius is calculated by using the formula:

$$r_t = 1.1019 \ ct^2$$

It is noted from above equations that the coordinate at any point is directly proportional to the thickness ratio and that the leading-edge radius varies as the square of the thickness ratio. Using the above equations the two dimensional airfoil are drawn and the figure 7 and figure 8 shows the airfoil i.e. un-morphed and Morphed respectively.
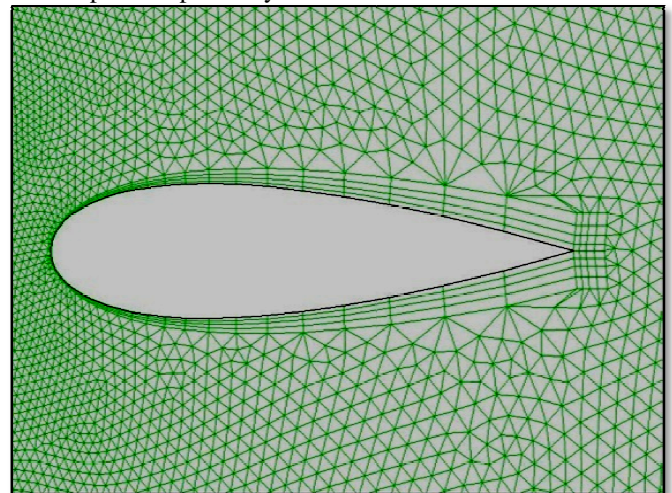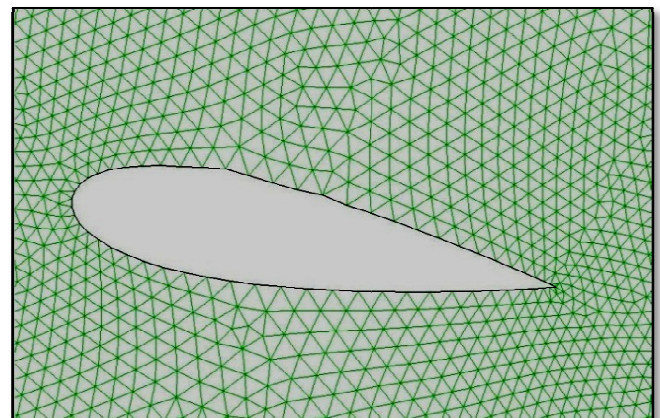

Figure-7
Un-morphed Airfoil

Figure-8
Morphed Airfoil

The CFD readings of airfoil un-morphed and Morphed can be calculated after the gambit design and fluent analysis. From the fluent analysis the coefficient of lift and coefficient of drag can be directly noted for different angle of attack.

Analytical Analysis: The analytical readings of airfoil un-morphed and Morphed can be calculated only by using the aerodynamic relatives[11]. For a symmetrical airfoil i.e. un-morphed the following relations can be used to calculate the coefficient of lift and coefficient of drag.

$$C_L = 2\pi\alpha \qquad\qquad C_D = 2\pi\alpha^2$$

For a unsymmetrical airfoil i.e. Morphed the following relations can be used to calculate the coefficient of lift and coefficient of drag[12].

$$C_L = 2\pi\alpha + C_{L0} \qquad\qquad C_D = (2\pi\alpha + C_{L0}) \times \alpha$$

Results and Discussion

Table 1 illustrate the experimental, CFD and analytical results for coefficient of lift and coefficient of drag on un-morphed and morphed airfoils at various angle of attack. The table 2 illustrates the lift to drag ratio achieved at various angle of attacks in experimental, CFD and analytical.

The figure 9, 10 and 11 illustrate the experimental, CFD and analytical analysis of both configuration wings. From the figure it is clear that for a morphing wing high lift is attained when compared to normal wing. At the zero angle of attack itself some amount of lift is attained and when the angle of attack increases the lift of morphing wing also increasing linearly and after 15˚ due to stalling the lift gets decreased but not less than the normal wing. The stalling angle is also increased when compared to un-morphed airfoil.

The figure 12 and figure 13 shows the pressure distribution over the both configuration wings at 20˚ angle of attack because of the stalling angle. From the figure 12 it is clear that the pressure on the lower surface of the airfoil is high and the pressure over the upper surface is low only at some region over the airfoil. But the figure 13 illustrates that pressure on the lower surface of the airfoil is slightly high and the pressure over the upper surface is very low for the entire surface. So from these figures it is clear that the lift obtained will be very high for morphed wing.

The figure 14 and figure 15 shows the velocity distribution over the both configuration wings. The figure 14 shows that the velocity distribution over the upper surface of airfoil trailing edge and lower surface of airfoil has very low velocity and velocity is maximum only at a small distance from the leading edge. But from the figure 14 illustrates the velocity is maximum for some more distance from the leading edge than the normal wing and on the lower surface of the airfoil the velocity is slightly higher than the normal wing.
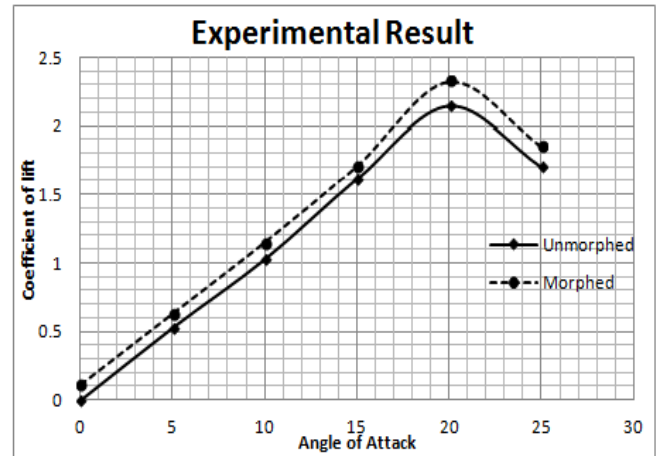

Figure-9
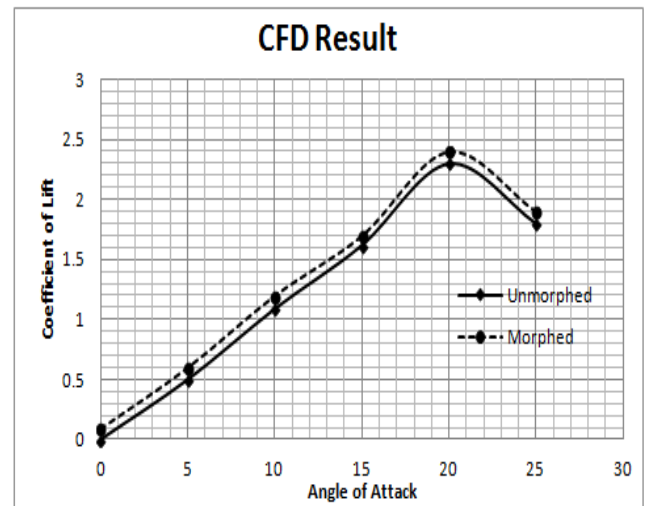**Angle of Attack vs. C_L (Experimental)**
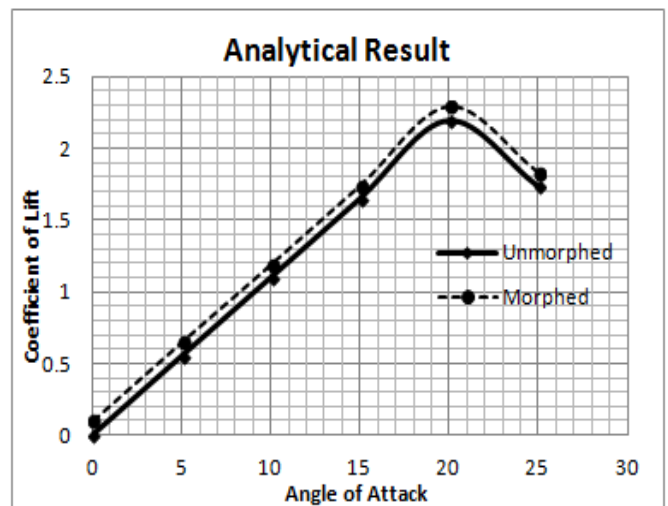

Figure-10
Angle of Attack vs. C_L (Numerical)

Figure-11
Angle of Attack vs. C_L (Analytical)
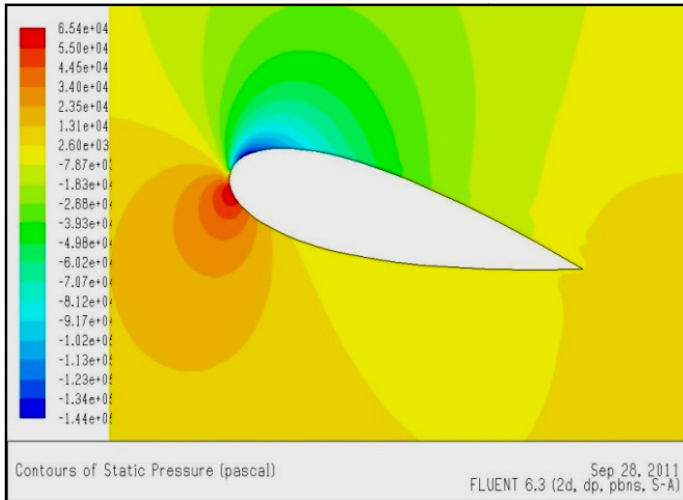
Figure-12
Pressure over Airfoil (Before Morphed)
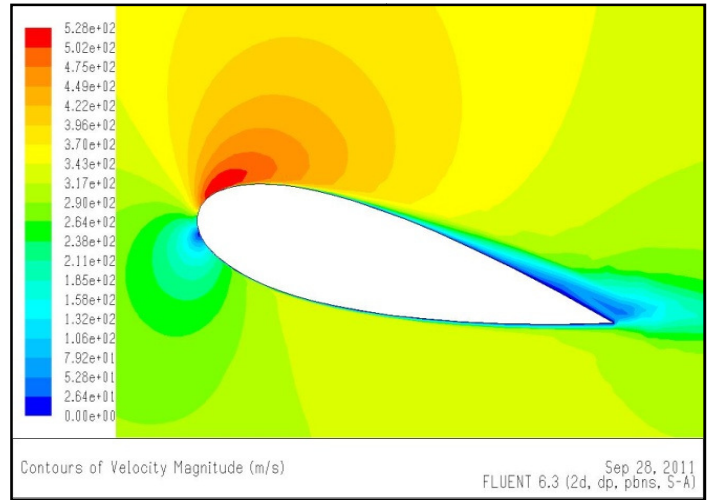

Figure-14
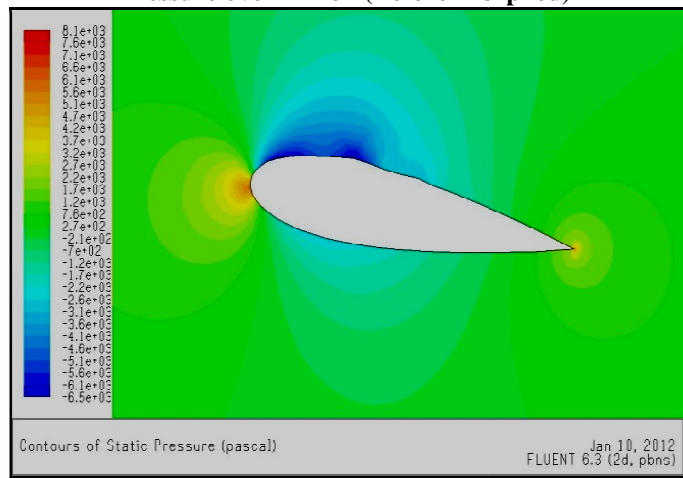**Velocity over Airfoil (Before Morphed)**

Figure-13
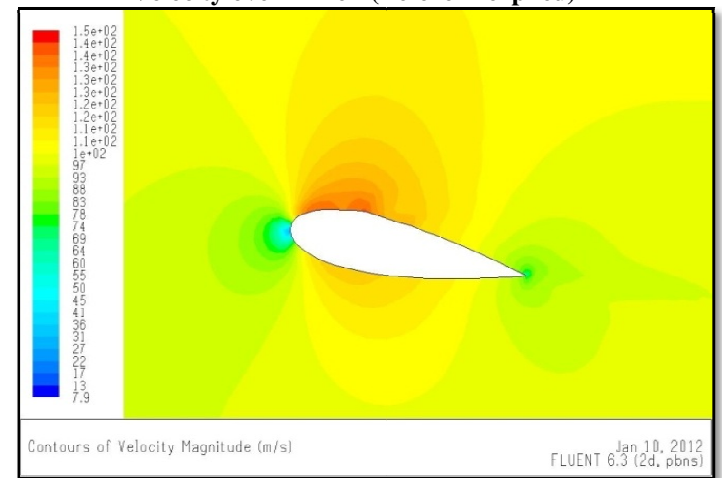**Pressure over Airfoil (After Morphed)**

Figure-15
Velocity over Airfoil (After Morphed)

Table-1
Experimental, CFD and analytical results of morphed and un-morphed

Angle of Attack (Deg)	Experimental				Numerical				Analytical			
	un-morphed		Morphed		un-morphed		Morphed		un-morphed		Morphed	
	C_L	C_D	C_L	C_D	C_L	C_D	C_L	C_D	C_L	C_D	C_L	C_D
0	0	0	0.11	0.009	0	0	0.09	0.011	0	0	0.1	0.011
5	0.53	0.07	0.63	0.052	0.5	0.05	0.6	0.05	0.55	0.06	0.65	0.057
10	1.03	0.24	1.15	0.19	1.09	0.22	1.2	0.20	1.096	0.242	1.19	0.21
15	1.62	0.53	1.71	0.42	1.62	0.5	1.7	0.45	1.644	0.55	1.74	0.46
20	2.15	0.97	2.33	0.73	2.3	0.93	2.4	0.80	2.190	0.978	2.29	0.79
25	1.71	0.59	1.85	0.63	1.8	0.57	1.9	0.65	1.735	0.61	1.83	0.7

Table-2
Result comparison of L/D ratio in experimental, numerical and analytical

Sl.No	Angle of Attack (Deg)	L/D Ratio					
		Experimental		Numerical		Analytical	
		Un-morphed	Morphed	Un-morphed	Morphed	Un-morphed	Morphed
1	0	0	12.2	0	8.2	0	9.09
2	5	7.57	12.12	10	12	9.17	11.46
3	10	4.29	6.05	4.95	6	4.5	5.75
4	15	3.05	4.07	3.24	3.78	2.98	3.83
5	20	2.22	3.19	2.47	3	2.23	2.87
6	25	2.89	2.94	3.16	2.93	2.83	2.6

Conclusion

The fabrication of morphing wing is equipped with new morphing actuation mechanism hardware with suitably designed controllers and the two-dimensional analysis, using computational fluid dynamics (CFD) and aerodynamic tests were conducted in an open-circuit wind tunnel for this morphing wing. The tests were carried out for this morphing wing and lift to drag ratio were determined at various angles of attack.

Then the results obtained by CFD and experimental have been discussed and these results show that the aerodynamic performance of the morphing wing configuration is prominent when compared to the conventional wing configuration. From the pressure distribution and velocity distribution diagrams it is clear that the morphing wing performance is prominent than the conventional wing configuration.

References

1. Mamou M., Mebarki Y., Khalid M. and Genest M., Aerodynamic performance optimization of a wind tunnel morphing wing model subject to various cruise flow conditions, *27th International congress of the aeronautical sciences,* (**ICAS 2010**)

2. Dayananda G.N., Senthil Kumar P. and Subba Rao M., Development of SMA based actuator mechanisms for deployment of control surfaces, *International Conference on Smart Materials Structures and Systems,* (**2005**)

3. Ermira J. Abdullah, Cees Bil and Simon Watkins, Testing of adaptive airfoil for UAV using shape memory alloy actuators, *27th International congress of the aeronautical sciences,* (**2010**)

4. Chi Seng LEE, Di-Bao WANG, Fei-Bin HSIAO, and Yen Hock LIM. Classification of airfoils by abnormal behavior of lift curves at low Reynolds number, *24th International congress of the aeronautical sciences* (**2004**)

5. Chi Seng LEE, Di-Bao WANG, Fei-Bin HSIAO, and Yen Hock LIM. Classification of airfoils by abnormal behavior of lift curves at low Reynolds number, *24th International congress of the aeronautical sciences* (**2004**)

6. Brian D., Roth and William A., Crossley, Application of optimization techniques in the conceptual design of morphing aircraft, *AIAA's 3rd Annual Aviation Technology, Integration, and Operations (ATIO) Tech* (**2003**)

7. Ming H. Wu and L. McD. Schetky, Industrial applications for shape memory alloys, Proceedings of the International Conference on Shape Memory and Super elastic Technologies, Pacific Grove, California, 171-182**, (2000)**

8. Jae-Sung Bae, Nam-Ho, Kyong T., Michael Seigler and Daniel J., *Aeroelastic Considerations on Shape Control of an Adaptive Wing, Korea Institute of Energy Research* (**2006**)

9. Yuvaraja M., Senthilkumar M, Balaguru I., Vibration Characteristics of A Gfrp Composite Beam Using SMA Actuator, *National Journal of Technology*, **7(4)** 11-17 (**2011**)

10. Thill C., Etches J., Bond I., Potter K. and P., Weaver, Morphing skins, *The aeronautical journal,* (**2008**)

11. John D. Anderson Jr., Fundamentals of Aerodynamics, Tata McGraw Hill Publishing Company Limited (**1991**)

12. Livier Gonzalez. Morphing wing using shape memory alloy: A conceptual proposal (**June 2002**)